Oxygen-Reduction Catalysts

DOI: 10.1002/anie.200907289

Nitrogen-Doped Ordered Mesoporous Graphitic Arrays with High Electrocatalytic Activity for Oxygen Reduction**

Ruili Liu, Dongqing Wu, Xinliang Feng, and Klaus Müllen**

The cathodic oxygen-reduction reaction (ORR) is one of the most crucial factors in the performance of a fuel cell.[1] The development of efficient ORR electrocatalysts is thus of great significance for the commercialization of fuel cells.[2] Platinum-based materials have long been investigated as active catalysts for ORR; however, the large-scale application of fuel cells has been hampered by the high cost and inadequacy of this metal.[3] Recently, nonprecious-metal[4] and metal-free catalysts[5] for ORR have attracted enormous interest as an alternative to platinum-based catalysts. In particular, nitrogen-doped carbon materials, which are typical metal-free catalysts, exhibit excellent electrocatalytic activity for ORR as a result of their unique electronic properties derived from the conjugation between the nitrogen lone-pair electrons and the graphene π system.[6] Generally, nitrogen-doped carbon materials can be prepared by the pyrolysis of transition-metal macrocyclic compounds[5a–f] or mixtures of metal salts and nitrogen-containing precursors.[5f–h] In these processes, the transition metals play an important role not only in the formation of graphitic frameworks, but also in the introduction of nitrogen active sites.[7] Drawbacks are the use of expensive precursors and the need for extra steps to remove metal species. Furthermore, metal nanoparticles encapsulated in the graphite framework still remain even after a tedious removal process. The nature of the nitrogen atoms in nitrogen-doped carbon materials and whether they are really the active catalytic sites is still controversial.[5f] Thus, the development of nitrogen-doped carbon materials with excellent electrochemical performance but without any metal components is an urgent issue. Such materials would not only be promising candidates for ORR catalysts but would aid attempts to elucidate the correlation between the structure, composition, and electrochemical activity of nitrogen-doped carbon materials.

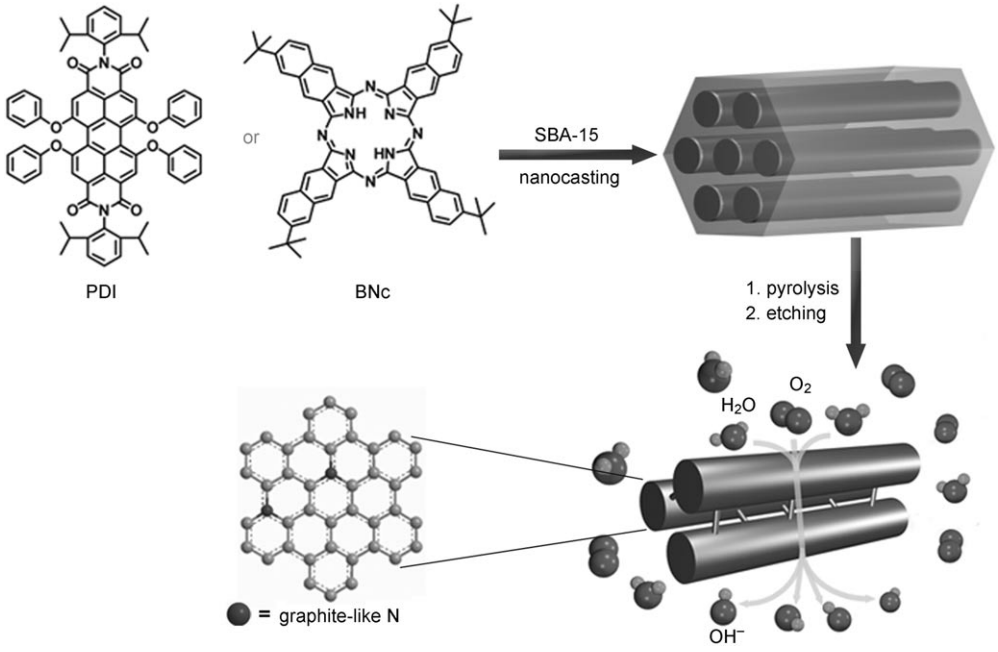

Figure 1. Preparation of NOMGAs as metal-free catalysts for the ORR.

Herein, we report the fabrication of novel nitrogen-doped ordered mesoporous graphitic arrays (NOMGAs) on the basis of a metal-free nanocasting technology. Ordered mesoporous silica SBA-15[8] was used as a template, and a nitrogen-containing aromatic dyestuff, *N*,*N*′-bis(2,6-diisopropyphenyl)-3,4,9,10-perylenetetracarboxylic diimide (PDI), was used as the carbon precursor (Figure 1). The unique features of the resulting NOMGAs, including a high surface area and a graphitic framework with a moderate nitrogen content, led to high electrocatalytic activity, excellent long-term stability, and resistance to crossover effects for the ORR. These properties were superior to those observed for the commercially available catalyst Pt–C. To the best of our

[*] Dr. R. Liu, Dr. D. Wu, Dr. X. Feng, Prof. Dr. K. Müllen
Max-Planck-Institut für Polymerforschung
Ackermannweg 10, 55128 Mainz (Germany)
Fax: (+49) 6131-379-350
E-mail: feng@mpip-mainz.mpg.de
muellen@mpip-mainz.mpg.de

[**] We thank Long Wang for TEM characterization and Dr. Chen Li for valuable discussions. This research was supported financially by the Max Plank Society through the program ENERCHEM, the German Science Foundation (Korean-German IRTG), and the DFG Priority Program SPP 1355.

Supporting information for this article is available on the WWW under http://dx.doi.org/10.1002/anie.200907289.

knowledge, such excellent electrochemical performance in the ORR has rarely been observed for metal-free catalysts.[5a] Owing to the metal-free preparation procedure, the electrocatalytic activity can be attributed exclusively to the incorporation of nitrogen in NOMGAs. A comparison of NOMGAs derived from different carbon precursors and formed at different pyrolysis temperatures suggests that graphite-like nitrogen atoms account for the excellent electrochemical performance in the ORR.

NOMGAs with different compositions were synthesized by the carbonization of PDI/SBA-15 composites at 600, 750, and 900 °C; the resulting materials are denoted as PDI-600, PDI-750, and PDI-900, respectively. The small-angle X-ray diffraction (XRD) pattern of PDI-900 showed three well-resolved diffraction peaks, which correspond to (100), (110), and (200) reflections of two-dimensional hexagonal arrangements (Figure 2A), and was similar to that of the material

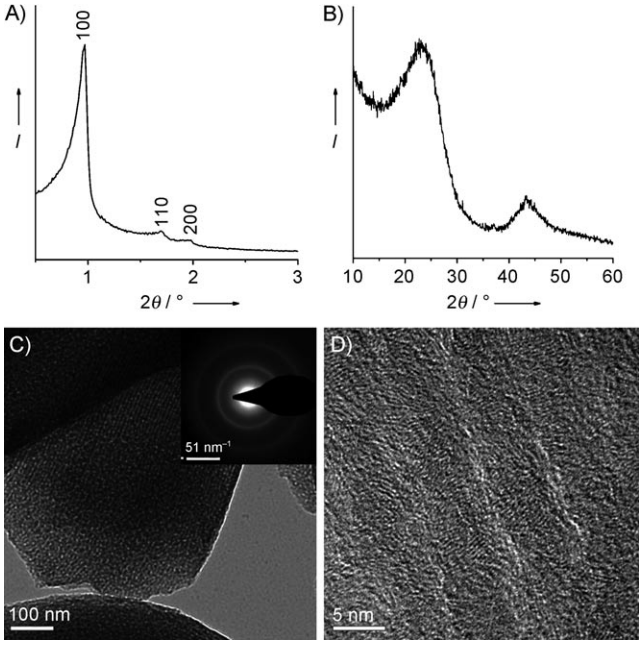

Figure 2. A) Small-angle and B) wide-angle XRD patterns of PDI-900; C) TEM and D) high-resolution TEM images of PDI-900. The inset in (C) is the SAED pattern.

CMK-3.[9] Transmission electron microscopy (TEM) confirmed the ordered mesostructure of PDI-900, as evidenced by large domains with well-ordered arrays of carbon rods and pore channels (Figure 2C). Furthermore, two broad peaks at $2\theta = 25$ and 43°, which correspond to (002) and (101) diffractions, were observed in the wide-angle XRD pattern of PDI-900 (Figure 2B). The *d* spacing (002) of around 0.36 nm is slightly larger than that of graphite (0.34 nm). The selected-area electron diffraction (SAED) pattern (inset in Figure 2C) showed clear diffraction rings, which suggested the formation of graphitic pore walls. A high-resolution TEM image (Figure 2D) further indicated the formation of crystalline frameworks and that the orientation of the graphite layers was perpendicular to the long axis (*c* axis) of the mesoporous carbon rods. Such a high graphitic degree and unique structure can be attributed to the highly ordered columnar stacking through π–π interactions and the general tendency towards an edge-on anchoring of disk-shaped molecules on inorganic walls.[10] The nitrogen sorption isotherm (see Figure S1 in the Supporting Information) revealed a type-IV adsorption curve with an H2-type hysteresis loop.[8] A very narrow pore-size distribution centered at about 3.8 nm was calculated from the adsorption branch on the basis of the Barrett–Joyner–Halenda (BJH) model. The Brunauer–Emmett–Teller (BET) surface area was about 510 $cm^2 g^{-1}$, and the total pore volume was 0.61 $cm^3 g^{-1}$. Elemental analysis revealed the following composition (wt %) of PDI-900: C 89.5, H 1.7, N 2.7, O (calculated) 6.1.

We compared the electrocatalytic properties of PDI-900 with those of commercial Pt–C (20 wt % platinum on Vulcan XC-72R). The same amount of each catalyst by mass (25.5 μg cm^{-2}) was loaded onto a glassy-carbon (GC) rotating-disk electrode (RDE) to give PDI-900/GC and Pt–C/GC, respectively. Figure 3A presents cyclic voltammogram (CV)

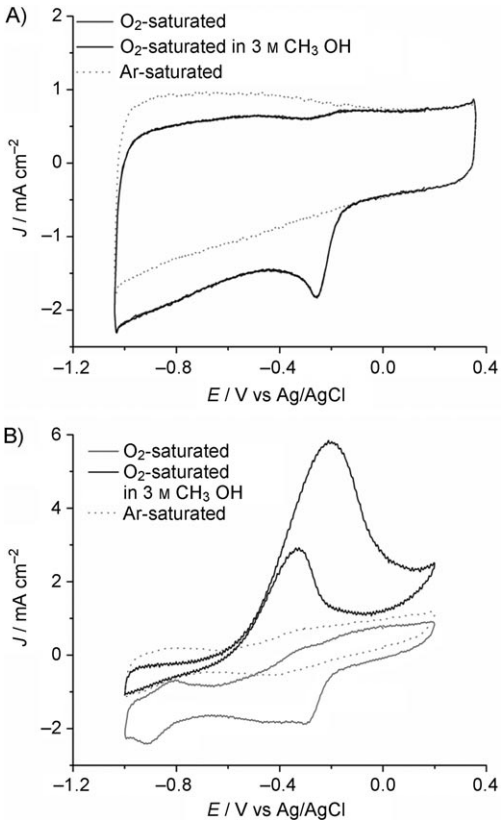

Figure 3. Cyclic voltammograms of A) PDI-900 and B) Pt–C on a glassy-carbon RDE electrode in an O_2-saturated 0.1 M solution of KOH, in an O_2-saturated 0.1 M solution of KOH upon the addition of CH_3OH (3 M) saturated with O_2, and in an argon-saturated 0.1 M solution of KOH.

curves of PDI-900/GC in 0.1M KOH solution saturated with argon or O_2 at a scan rate of 100 mV s^{-1}. Featureless voltammetric currents within the potential range between −1.0 and +0.2 V were observed for PDI-900/GC in the argon-saturated solution (dotted curve). In contrast, when the

electrolyte solution was saturated with O_2, the reduction current appeared as a well-defined cathodic peak at −0.26 V, which suggests pronounced electrocatalytic activity of PDI-900/GC for oxygen reduction. To examine possible crossover effects, we measured the electrocatalytic selectivity of PDI-900/GC and Pt–C/GC against the electrooxidation of methanol (a common fuel molecule) in O_2-saturated 0.1 M KOH in the presence of methanol (3.0 M). One pair of peaks, at −0.35 and −0.20 V, were observed for methanol oxidation in the CV curve for Pt–C/GC, whereas the cathodic peak for ORR had vanished (Figure 3B). In contrast, no noticeable change was observed in the oxygen-reduction current on PDI-900/GC under the same conditions (Figure 3A). Thus, PDI-900/GC exhibited high selectivity for ORR with a remarkably good ability to avoid crossover effects and outperformed the Pt–C/GC electrode. This material holds high promise for use in direct methanol and alkaline fuel cells.

To gain further insight into the role of PDI-900/GC during the ORR electrochemical process, we studied the reaction kinetics by rotating-disk voltammetry. The voltammetric profiles in O_2-saturated 0.1 M KOH as the electrolyte showed that the current density was enhanced by an increase in the rotation rate (from 400 to 3600 rpm; Figure 4A). The onset potential of PDI-900/GC for ORR was at approximately −0.13 V, close to that identified from CV measurements (−0.12 V; Figure 3A). The corresponding Koutecky–Levich plots (J^{-1} vs $\omega^{-1/2}$) at various electrode potentials exhibited good linearity (Figure 4B). The slopes remain approximately constant over the potential range from −0.25 to −0.40 V, which suggests that the electron transfer numbers for oxygen reduction at different electrode potentials are similar. Linearity and parallelism of the plots are usually taken as an indication of first-order reaction kinetics with respect to the concentration of dissolved O_2. The kinetic parameters can be analyzed on the basis of the Koutecky–Levich equations [Eqs. (1)–(3)][11]:

$$\frac{1}{J}=\frac{1}{J_L}+\frac{1}{J_K}=\frac{1}{B\omega^{1/2}}+\frac{1}{J_K} \quad (1)$$

$$B=0.62nFC_0(D_0)^{2/3}\nu^{-1/6} \quad (2)$$

$$J_K=nFkC_0 \quad (3)$$

in which J is the measured current density, J_K and J_L are the kinetic- and diffusion-limiting current densities, ω is the angular velocity of the disk ($\omega=2\pi N$, N is the linear rotation speed), n is the overall number of electrons transferred in oxygen reduction, F is the Faraday constant ($F=96485\ \mathrm{C\,mol^{-1}}$), C_0 is the bulk concentration of O_2, ν is the kinematic viscosity of the electrolyte, and k is the electron-transfer rate constant. According to Equations (1) and (2), the number of electrons transferred (n) and J_K can be obtained from the slope and intercept of the Koutecky–Levich plots, respectively. By using the values $C_0=1.2\times10^{-3}\ \mathrm{mol\,L^{-1}}$, $D_o=1.9\times10^{-5}\ \mathrm{cm\,s^{-1}}$,

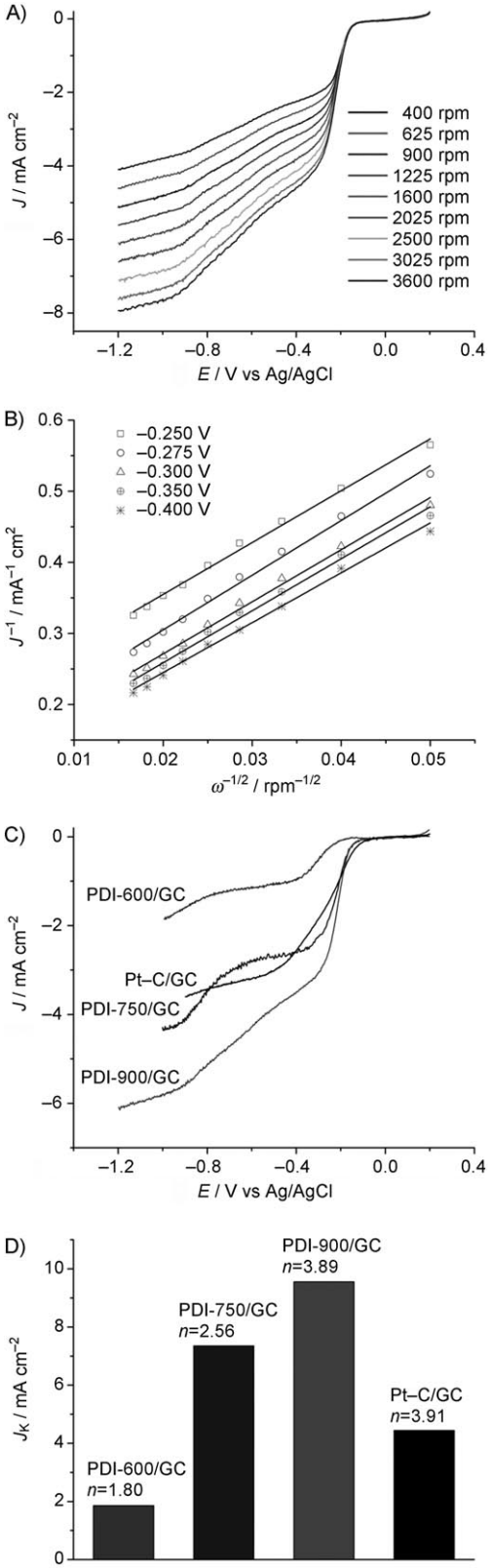

Figure 4. A) Rotating-disk voltammograms recorded for PDI-900 supported on a GC electrode in an O_2-saturated 0.1 M solution of KOH at a scan rate of 10 $\mathrm{mV\,s^{-1}}$ and different rotation rates. B) Koutecky–Levich plot of J^{-1} versus $\omega^{-1/2}$ at different electrode potentials. The experimental data were obtained from (A); the lines are linear regressions. C) RDE voltammograms of the series of PDI-NOGMAs and Pt–C supported on GC electrodes at a rotation rate of 1600 rpm. The experimental conditions are the same as in (A). D) Electrochemical activity given as the kinetic-limiting current density (J_K) at −0.35 V for the PDI-NOGMAs supported on GC electrodes in comparison with that of a commercial Pt–C electrode.

and $v = 0.1\ m^2 s^{-1}$ in 0.1 M KOH,[11b] n was calculated to be 3.89 at −0.35 V. This result suggests that PDI-900 leads to a four-electron transfer in oxygen reduction. The calculated J_K value of 9.15 mA cm^{-2} at −0.35 V is more than twice as high as that of commercially available Pt–C/GC (4.44 mA cm^{-2} at −0.35 V; Figure 4D).

As discussed above, the NOMGAs fabricated from the PDI precursor (denoted as PDI-NOMGAs) originate from a metal-free process, which enables a firm correlation between their mesostructure characteristics and electrochemical performance. Thus, we further investigated the effects of the carbonization temperature (600, 750, and 900 °C) of the PDI-NOMGAs on their electrocatalytic activity. As described for PDI-900/GC, PDI-600 and PDI-750 were supported on a glassy-carbon RDE to give PDI-600/GC and PDI-750/GC, respectively. The rotating-disk voltammograms in O_2-saturated 0.1 M KOH solution at a rotation rate of 1600 rpm are compared in Figure 4C. Both PDI-600/GC and PDI-750/GC showed a two-step process for ORR, with the onset potential at −0.23 and −0.75 V for the former and −0.15 and −0.71 V for the latter. This result suggests that their reduction processes favor a two-electron over a four-electron pathway ($n = 1.80$ and 2.56 were calculated for PDI-600/GC and PDI-750/GC, respectively). Furthermore, linear regressions on the basis of the Koutecky–Levich equations showed that an increase in the pyrolysis temperature led to a clear enhancement of the electron-transfer kinetics of oxygen reduction, as reflected by kinetic-limiting current densities (J_K; Figure 4D). Therefore, PDI-600 and PDI-750, with a higher nitrogen content than that of PDI-900, actually exhibited lower selectivity and catalytic activity, which indicates that the nitrogen content does not directly affect the electrochemical performance. When NOMGAs were prepared from another nitrogen-rich aromatic molecule, tetrakis(*tert*-butyl)naphthalocyanine (BNc; Figure 1), the higher nitrogen content in these BNc-NOMGAs (6.8–3.5 wt %, as determined by elemental analysis) also did not result in improved activity.

We employed X-ray photoelectron spectroscopy (XPS) to analyze further the chemical state of the carbon and nitrogen atoms within the carbon frameworks. Again we used the series of PDI-NOMGAs to evaluate the effect of the pyrolysis temperature on the composition of the materials. The C 1s peaks for the PDI-NOMGA series (see Figure S2A in the Supporting Information) were centered at approximately 285.0 eV (continuation of sp^2 graphitic carbon) and were slightly asymmetric, which is a common effect for nitrogen-doped carbon materials.[12] The half-peak width of the C 1s spectra became narrower as the pyrolysis temperature increased. A narrower half-peak width suggests an enhanced graphitic character. This connection was further supported by Raman spectra (see Figure S3 in the Supporting Information), in which the G band became significantly sharper, and the intensity ratio of the G to the D band increased at higher pyrolysis temperatures.[13] The complex XPS N 1s spectra (see Figure S2B in the Supporting Information) were fitted to three components of the binding energy: that due to pyridine-like nitrogen atoms (398.4 eV), graphite-like nitrogen atoms (401.3 eV), and pyridine *N*-oxide (403.0 eV).[5g] The pyridine-like nitrogen atoms can be transformed into graphite-like nitrogen atoms at higher pyrolysis temperatures,[14] albeit with a decrease in the overall nitrogen content from 3.5 to 2.7 wt % for PDI-NOMGAs (see Table 1 and Figure S2B in the Supporting Information). Since the PDI-NOMGAs obtained at different pyrolysis temperatures have almost identical mesostructures (see Table S1 in the Supporting Information), the significantly enhanced activity and selectivity of PDI-900 must be attributed to the combination of the highly graphitic degree of this material and the increased proportion of graphite-like nitrogen atoms (see Table S1 and Figure S2B in the Supporting Information). The importance of the latter aspect was confirmed by comparing PDI-NOMGAs with BNc-NOMGAs pyrolyzed at the same temperature (see Table S1 in the Supporting Information). This conclusion is further supported by both experimental results[5c] and computational studies.[6]

Since durability is one of the major concerns in current fuel-cell technology, the stability of PDI-900/GC was further tested at a constant voltage of −0.26 V for 20000 s in an 0.1 M KOH solution saturated with O_2 at a rotation rate of 1600 rpm (Figure 5). Remarkably, the corresponding current–time (i–t) chronoamperometric response of PDI-900/GC exhibited a very slow attenuation after a fast decrease of 10 % within the first 3000 s, and a high relative current of 84.7 % still persisted after 20000 s. In contrast, Pt–C/GC showed a gradual decrease with a current loss of approximately 52.0 % measured after 20000 s. This result suggests that the durability of PDI-900 is superior to that of the Pt–C catalyst.

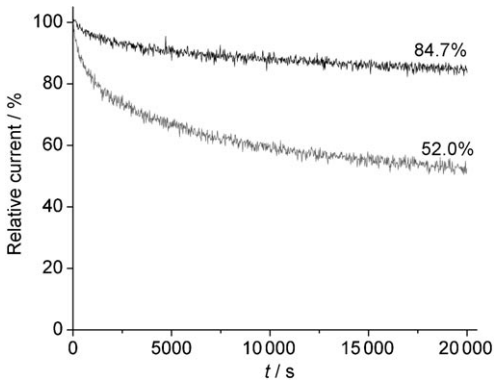

Figure 5. Current–time (i–t) chronoamperometric response of PDI-900- and Pt–C-modified GC electrodes at −0.26 V in O_2-saturated 0.1 M KOH at a rotation rate of 1600 rpm.

In conclusion, we have demonstrated the fabrication of novel NOMGAs by a simple, cost-effective, and readily reproducible approach. The resulting nitrogen-doped carbon materials serve as true metal-free catalysts that show outstanding electrocatalytic activity, long-term stability, and excellent resistance to crossover effects for ORR. Furthermore, our study indicates that graphite-like nitrogen atoms in NOMGAs play a crucial role for oxygen reduction. With this synthetic approach, nitrogen-doped carbon materials with a high proportion of graphite-like nitrogen atoms can be

prepared by rationally selecting nitrogen-rich aromatic precursors to yield metal-free catalysts with enhanced electrochemical performance.

Received: December 26, 2009
Published online: March 9, 2010

Keywords: electrocatalysts · fuel cells · metal-free catalysts · nitrogen-doped carbon · oxygen reduction

[1] B. C. H. Steele, A. Heinzel, *Nature* **2001**, *414*, 345.
[2] a) B. Sljukic, C. E. Banks, R. G. Compton, *J. Iran. Chem. Soc.* **2005**, *2*, 1; b) *Recent Trends in Fuel Cell Science and Technology* (Ed: S. Basu), Springer, New York, **2007**.
[3] a) M. Winter, R. J. Brodd, *Chem. Rev.* **2004**, *104*, 4245; b) X. W. Yu, S. Y. Ye, *J. Power Sources* **2007**, *172*, 145; c) Z. W. Chen, M. Waje, W. Z. Li, Y. S. Yan, *Angew. Chem.* **2007**, *119*, 4138; *Angew. Chem. Int. Ed.* **2007**, *46*, 4060; d) B. Lim, M. J. Jiang, P. H. C. Camargo, E. C. Cho, J. Tao, X. M. Lu, Y. M. Zhu, Y. N. Xia, *Science* **2009**, *324*, 1302.
[4] a) R. Jasinski, *Nature* **1964**, *201*, 1212; b) R. Bashyam, P. Zelenay, *Nature* **2006**, *443*, 63; c) M. Lefèvre, E. Proietti, F. Jaouen, J.-P. Dodelet, *Science* **2009**, *324*, 71; d) *N4-Macrocyclic Metal Complexes* (Eds.: J. H. Zagal, F. Bedioui, J.-P. Dodelet), Springer, New York, **2006**; e) C. W. B. Bezerra, L. Zhang, K. C. Lee, H. S. Liu, A. L. B. Marques, E. P. Marques, H. J. Wang, J. J. Zhang, *Electrochim. Acta* **2008**, *53*, 4937.
[5] a) K. P. Gong, F. Du, Z. H. Xia, M. Durstock, L. M. Dai, *Science* **2009**, *323*, 760; b) Y. Tang, B. L. Allen, D. R. Kauffman, A. Star, *J. Am. Chem. Soc.* **2009**, *131*, 13200; c) H. Niwa, K. Horiba, Y. Harada, M. Oshima, T. Ikeda, K. Terakura, J. Ozaki, S. Miyata, *J. Power Sources* **2009**, *187*, 93; d) T. Iwazaki, R. Obinata, W. Sugimoto, Y. Takasu, *Electrochem. Commun.* **2009**, *11*, 376; e) E. J. Biddinger, D. von Deak, U. S. Ozkan, *Top. Catal.* **2009**, *52*, 1566; f) Y. Y. Shao, J. H. Sui, G. P. Yin, Y. Z. Gao, *Appl. Catal. B* **2008**, *79*, 89; g) P. H. Matter, L. Zhang, U. S. Ozkan, *J. Catal.* **2006**, *239*, 83; h) E. J. Biddinger, D. von Deak, U. S. Ozkan, *Top. Catal.* **2009**, *52*, 1566.
[6] a) R. A. Sidik, A. B. Anderson, N. P. Subramanian, S. P. Kumaraguru, B. N. Popov, *J. Phys. Chem. B* **2006**, *110*, 1787; b) K. A. Kurak, A. B. Anderson, *J. Phys. Chem. C* **2009**, *113*, 6730; c) T. Ikeda, M. Boero, S. F. Huang, K. Terakura, M. Oshima, J. Ozaki, *J. Phys. Chem. C* **2008**, *112*, 14706; d) L. S. Panchakarla, K. S. Subrahmanyam, S. K. Saha, A. Govindaraj, H. R. Krishnamurthy, U. V. Waghmare, C. N. R. Rao, *Adv. Mater.* **2009**, *21*, 4726.
[7] a) E. Yeager, *Electrochim. Acta* **1984**, *29*, 1527; b) K. Wiesener, *Electrochim. Acta* **1986**, *31*, 1073; c) S. Maldonado, K. J. Stevenson, *J. Phys. Chem. B* **2005**, *109*, 4707.
[8] D. Y. Zhao, Q. S. Huo, J. L. Feng, B. F. Chmelka, G. D. Stucky, *J. Am. Chem. Soc.* **1998**, *120*, 6024.
[9] S. Jun, S. H. Joo, R. Ryoo, M. Kruk, M. Jaroniec, Z. Liu, T. Ohsuna, O. Terasaki, *J. Am. Chem. Soc.* **2000**, *122*, 10712.
[10] a) L. J. Zhi, T. Gorelik, J. S. Wu, U. Kolb, K. Müllen, *J. Am. Chem. Soc.* **2005**, *127*, 12792; b) L. J. Zhi, J. S. Wu, J. X. Li, U. Kolb, K. Müllen, *Angew. Chem.* **2005**, *117*, 2158; *Angew. Chem. Int. Ed.* **2005**, *44*, 2120.
[11] a) A. J. Bard, L. R. Faulkner, *Electrochemical Methods: Fundamentals and Applications*, Wiley, New York, **2001**; b) W. Chen, S. W. Chen, *Angew. Chem.* **2009**, *121*, 4450; *Angew. Chem. Int. Ed.* **2009**, *48*, 4386.
[12] R. Côté, G. Lalande, D. Guay, J. P. Dodelet, G. Dénès, *J. Electrochem. Soc.* **1998**, *145*, 2411.
[13] T. W. Kim, I. S. Park, R. Ryoo, *Angew. Chem.* **2003**, *115*, 4511; *Angew. Chem. Int. Ed.* **2003**, *42*, 4375.
[14] J. R. Pels, F. Kapteijn, J. A. Moulijn, Q. Zhu, K. M. Thomas, *Carbon* **1995**, *33*, 1641.

